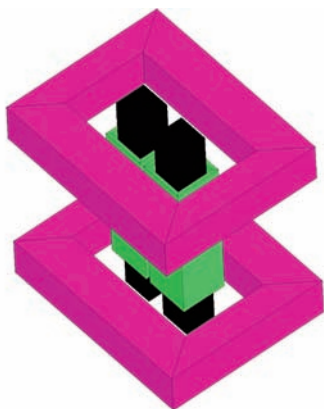
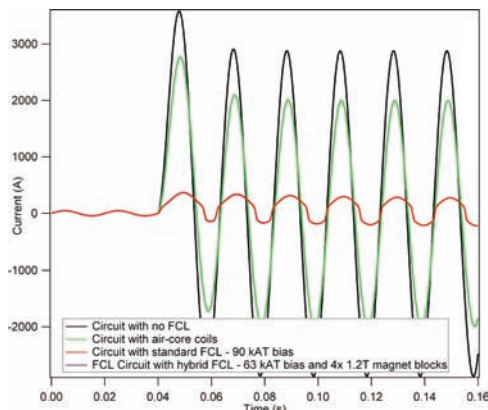


commercial-scale FCLs that can be biased with a DC-coil/permanent-magnet hybrid, rather than the currently used superconducting coils.

[1] J.-L. Rasolonjanahary, J. Sturgess, E. Chong, A. Baker, and C. Sasse, "Design and construction of a magnetic fault current limiter," in *Power Electronics, Machines and Drives*, 2006. The 3rd IET International Conference on, mar. 2006, pp. 681–685. [2] H. Schmitt, "Fault current limiters report on the activities of cigre wg a3.16," in *Power Engineering Society General Meeting*, 2006. IEEE, 0-0 2006, p. 5 pp.



Basic configuration of a single-phase saturated-core FCL



Fault clipping performance of both FCL designs compared with no FCL or an air-core reactor

2:30

HE-04. Efficient Magnetically Coupled Wireless Power Supply for Medical Implants with a High Tolerance to Coupling Coefficient Drift. A. Czarnecki^{1,2}, B.L. Mclaughlin², N. Sun¹ and A.L. Kindle². *EECE, Northeastern University, Boston, MA; 2. CS Draper Laboratory, Cambridge, MA*

Implanted medical devices such as cochlear implants are often powered wirelessly through the skin by resonant magnetic coupling [1]. Previously reported work derives the power transfer efficiency from a linear circuit model of mutual inductance [2,3]. However in a real-world system, real-time variations in coupling coefficient arise from mechanical movement resulting in an unstable transfer-function [4]. We propose a system to minimize power loss in the inductive coupling link by using an efficient switching voltage regulator on the implant in combination with closed loop control of the source voltage. Figure 1 shows the proposed inductive coupling circuit. A switching voltage regulator between the secondary inductor and the load buffers the load circuit from the effect of unstable coupling coefficient. This allows the load circuit to receive constant power regardless of the time varying coupling coefficient. The input to the switching regulator is modeled as a non-linear equivalent AC resistance. The equivalent circuit is solved in the phasor

domain at the system operating frequency. Because the equivalent load resistance is non-linear, the power transfer efficiency is dependent on source voltage. This is in contrast to the previously reported linear circuit model where power transfer efficiency is independent of source voltage. Figure 2 shows the overall power coupling efficiency to a constant power load as a function of the source voltage. There is a single optimal source voltage that results in peak efficiency for any given coupling coefficient. Also the value of the optimal source voltage varies with changes in the coupling coefficient. Because of this it is necessary to implement closed loop control of the source voltage to maintain peak efficiency in the face of a varying coupling coefficient.

[1] S. Rebscher and W. V. Harrison, "Cochlear Implants: System Design, Integration and Evaluation," pp. 115-142, 2009. [2] M. W. Baker, S. Member, and R. Sarpeshkar, "Feedback Analysis and Design of RF Power Links for Low-Power Bionic Systems," *IEEE Transactions on Biomedical Circuits and Systems*, vol. 1, no. 1, pp. 28-38, 2007. [3] R. R. Harrison, "Designing Efficient Inductive Power Links for Implantable Devices," 2007 IEEE International Symposium on Circuits and Systems, no. 2, pp. 2080-2083, May 2007. [4] R. Bashirullah, M. Sivaprakasam, G. a. Kendir, M. S. Humayun, and J. D. Weiland, "A closed loop transcutaneous power transfer system for implantable devices with enhanced stability," 2004 IEEE International Symposium on Circuits and Systems (IEEE Cat. No.04CH37512), pp. IV-17-20.

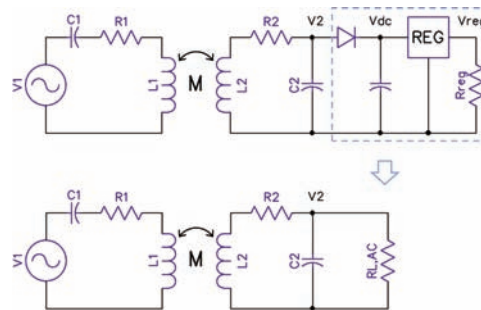


Fig. 1: Schematic of an inductive coupling circuit with a rectifier and switching regulator. Also shown is the AC equivalent circuit.

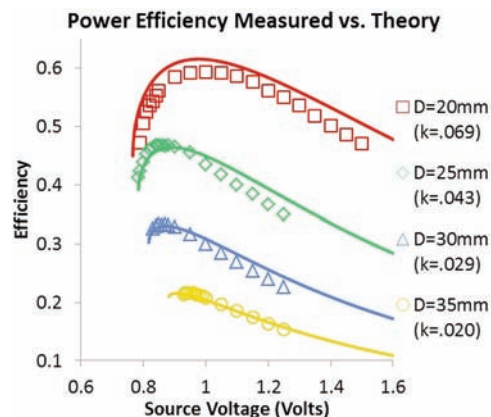


Fig. 2: Calculated (solid line) and measured power coupling efficiency as a function of source voltage is plotted at four different coupling coefficients (k) corresponding to four different coil separation distances (D) between the two inductors.

2:42

HE-05. Design of a transverse flux machine for power generation from seawaves. A. Viola¹, V. Franzitta¹ and M. Trapanese². *Dipartimento di Ingegneria dell'Energia, Palermo University, Palermo, Italy; 2. Dipartimento di Ingegneria Elettrica, Palermo University, Palermo, Italy*

Linear electrical generator has been recently studied for the exploitation of sea wave energy, however the definition of the optimum geometry to be used

is still debated and due to the fact that seawave energy is characterized by low speed and very high forces, a generator which is able to convert energy at low speed and high force is needed. In this paper we investigate the possibility to use a transverse flux linear generator (TFG) because transverse flux technology presents the highest force density per volume index among the iron based electrical machines. The advantages of TFG topology against the classical longitudinal concept are [1]: (a) the magnetomotive force per pole is independent from the total pole numbers; (b) the magnetic flux geometry and the coil section are independent design parameters; (c) armature coils geometry is simple; (d) phases are magnetically decoupled. Exploiting this advantages we have designed a TFG for power generation from seawaves. Since the TFM's flux path is intrinsically 3D, a 3D finite element analyses has been used to design the motor. In order to optimize the design, several simulations were done assuming well defined constraints. In each simulation the electrical and geometrical parameters of the generator were varied and rotor was supposed to be acted by a water wave train. The wave train consisted of ten oscillations. Each oscillation of the train wave had an amplitude and a frequency generated through a random number generator whose statistic features were obtained from the experimental data of actual seawaves. The objective function was the maximization of energy output and the constraints were the volume of iron to be used. This approach leads to determine a well defined geometry of TFG. This geometry has been used to numerically simulate the generated electromotive force, the power output, and to evaluate the maximum mechanical stress on the generators parts.

[1] J. S. D. Garcia., M. V. F. da Luz, J. P. A. Bastos, N. Sadowski, " Transverse Flux Machines: What for?", IEEE Multidisc Eng Educ Mag, Vol. 2, No. 1, March 2007

2:54

HE-06. Batch Magnetic Patterning of Hard Magnetic Films Using

Pulsed Magnetic Fields and Soft Magnetizing Heads. O.D. Oniku¹, R. Regojo¹, W.C. Patterson¹, K. Steiner¹ and D.P. Arnold¹. *Electrical and Computer Engineering, University of Florida, Gainesville, FL*

We report a method to impart spatially defined magnetic patterns into contiguous hard magnetic films using pulsed magnetic fields. Differing from most prior investigations [1-3], we use a pulsed magnetic field from an external electromagnet and a single magnetizing head rather than a sandwich structure. This approach facilitates batch-magnetizing over large surface areas and can potentially be scaled to dimensions $\ll 1$ mm. To demonstrate the concept, an array of 250- μm -wide magnetic stripes with alternating polarity is patterned in an 18- μm -thick Co-rich CoPt (Co₈₀Pt₂₀) film using a structured FeCo magnetizing head. The magnetically hard Co₈₀Pt₂₀ film ($B_r = 1$ T, $H_{ci} = 330$ kA/m, $BH_{max} = 130$ kJ/m³ out-of-plane) is electroplated on a Si substrate using the methods described in [4-5]. The magnetizing head is prepared by machining an array of 250 μm wide teeth (aspect ratio=1) in a bulk FeCo material. The process begins by pre-magnetizing the CoPt sample in the "up" direction using a ~ 3 T pulsed field. Fig. 1 illustrates the selective magnetic patterning process. The magnetizing head is brought into contact with the CoPt film, and a pulsed magnetizing field is applied to the two pieces in the "down" direction. Due to the field concentrating effect of the magnetizing head, the regions of the CoPt film that are in contact with the FeCo teeth are subjected to a stronger field. By adjusting the magnitude of this reversal field (~ 0.3 T in the experiments here), selective areas of the film are magnetized "down", while the other areas retain their previous "up" magnetization. As shown in Fig. 2, the resulting field pattern is measured 20 μm above the film surface using a precision scanning Hall probe ($1 \mu\text{m} \times 1 \mu\text{m}$ square active area), demonstrating that an alternating field of desired pole-width has been achieved. Achieving fine pole-pitch patterns are highly relevant for microscale electric machines, lab-on-a-chip devices, magnetic undulators, and many other applications.

(1) J. Topfer, B. Pawlowski, H. Beer, et. al., "Multi-pole magnetization of NdFeB magnets for magnetic micro-actuators and its characterization with a magnetic field mapping device", J. Magn. Magn. Mater., 270 (2004) 124-

129 (2) J. Topfer and V. Christoph, "Multi-pole magnetization of NdFeB sintered magnets and thick films for magnetic micro-actuators", Sensors and Actuators A, 113 (2004), 257-263 (3) I. Zana, F. Herrault, D. P. Arnold and M. G. Allen, "Magnetic patterning of permanent-magnet rotors for microscale motors/generators", Tech. Dig. 5th Int. Workshop for Power Generation and Energy Conversion Apps., Tokyo, Japan, pp. 116-119, November, 2005 (4) N. Wang and D. P. Arnold, "Thick Electroplated Co-rich CoPt Micromagnet Arrays for Magnetic MEMS", IEEE Trans. Magn., vol. 44, pp. 3969-3972, November 2008 (5) O. D. Oniku and D. P. Arnold, "Microfabrication of high performance thick Co₈₀Pt₂₀ permanent magnets for microsystems applications", Accepted for publication in ECS Transactions, September 2012

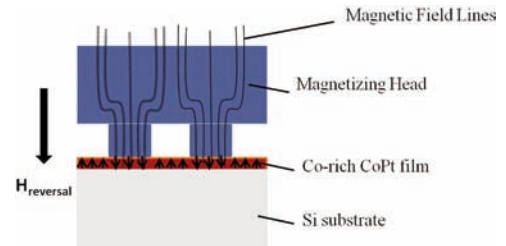


Fig. 1: Illustration of selective magnetic patterning

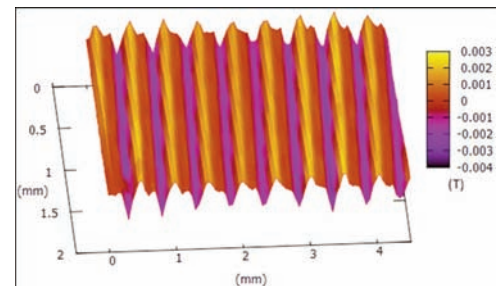


Fig. 2: Magnetic field pattern 20 μm above the CoPt film surface

3:06

HE-07. Steering of Magnetic Micro-swimmers.

Y. Li¹, H. Lin¹ and C. Chen¹. *National Chiao Tung University, Hsinchu, Taiwan*

We experimentally investigate the motion of a micro-swimmer consisting of several magnetic particles with different sizes. The swimmer is firstly formed by a static unidirectional field (H_d), and then manipulated by an additional oscillating field (H_p). Due to the asymmetric oscillating motion, the micro-swimmer generates thrust to move toward the direction of its center of mass (larger particles). It is known that such magnetic particle swimmers (or chains) driven by an external field would oscillate with the orientation of the field but lagging behind by certain phase angles. In this work, we demonstrate if a swimmer subjected to a strong oscillating field which results in an instantaneous phase lag (denoted as $\Delta\theta_L$) greater than 90° , an interesting phenomenon of reverse oscillation is observed. Consequently, instead of a concurrent oscillation with the external field, the swimmer oscillates reversely to steer perpendicularly to its original direction. Demonstrated in the figure are sequential images of steering behaviors of a swimmer consisting of two small and two large particles (denoted as S2L2). The mechanism of such steering behaviors can be understood by the induced magnetic torque (M) given as $M \sim \sin(2\Delta\theta_L)$. The magnetic torque changes sign when $|\Delta\theta_L| > 90^\circ$, so that the chain would start to oscillate oppositely to the original external field. Nevertheless, when the lagging phase angle reduces to $|\Delta\theta_L| < 90^\circ$, the magnetic torque would change sign again, and the chain resumes to its original oscillating trajectory. Steering of a micro-swimmer can be effectively manipulated by varying the field strength, which directly affects $\Delta\theta_L$.